



**Repositorio Institucional de la Universidad Autónoma de Madrid**

<https://repositorio.uam.es>

Esta es la **versión de autor** del artículo publicado en:  
This is an **author produced version** of a paper published in:

Journal of Alzheimer's Disease 45.1 (2015): 1-14

**DOI:** 10.3233/JAD-140456

**Copyright:** © 2015 IOS Press

El acceso a la versión del editor puede requerir la suscripción del recurso  
Access to the published version may require subscription

# Cathepsin D in a Murine Model of Frontotemporal Dementia with Parkinsonism-Linked to Chromosome 17

Julia Fernández-Montoya and Mar Pérez\*

Departamento de Anatomía, Histología y Neurociencia, Facultad de Medicina,  
Universidad Autónoma de Madrid,

Madrid, Spain

Accepted 4 November 2014

**Abstract.** Tauopathies, such as Alzheimer's disease (AD) and Frontotemporal dementia with Parkinsonism linked to chromosome 17 (FTDP-17), are characterized by tau accumulation. This accumulation could result from alterations in tau degradation by either the ubiquitin-proteasome system or the autophagy-lysosomal pathway. To analyze a possible alteration of the autophagy-lysosomal pathway in transgenic mice expressing human tau with three FTDP-17 missense mutations (TauVLW mice), we studied the lysosomal enzyme Cathepsin D. The hippocampi of TauVLW mice, where the human mutant tau accumulates, showed both increased Cathepsin D and partial colocalization of Cathepsin D with human mutant tau. At the ultrastructural level, some multivesicular bodies showed human mutant tau-immunopositive vesicles. This finding could provide insights into the molecular mechanisms of tau degradation in human tauopathies.

**Keywords:** Cathepsin D, FTDP-17, lysosomal system, mutated tau

## INTRODUCTION

Tau is an axonal cytosolic protein whose best known function is to promote microtubule assembly and stabilization [1]. However, accumulation of aggregated insoluble tau is a hallmark of many neurodegenerative diseases, including Alzheimer's disease (AD), progressive supranuclear palsy, and Frontotemporal dementia with Parkinsonism linked to chromosome 17 (FTDP-17). Collectively, these disorders are referred to as tauopathies [2]. Since tau inclusions are a feature of tauopathies, tau processing has been examined extensively in both in vitro and in vivo models. The investigations have focused either on post-translational modification of tau [3] or on mechanisms of tau degradation [4].

Two major proteolytic systems contribute to tau degradation inside cells, the ubiquitin-proteasome system and the autophagy-lysosomal system [4, 5]. Indeed, as it does for other proteins, proteasome/ubiquitin-proteasome may degrade natively-unfolded tau. Many studies have proposed increased lysosomal function as a strategy for reducing protein accumulation in age-related disorders [6]. Although tau clearance probably occurs through different mechanisms, there are some

experimental evidences supporting tau degradation in lysosomes [7–9] and thus lysosomal dysfunction could also induce tau pathology [10].

Under normal conditions, the lysosomal system serves as an important site for intracellular protein turnover and proteolytic processing of certain proteins mediated by lysosomal hydrolases called cathepsins. Cathepsins are lysosomal proteases whose enzymatic activity is conferred by critical residues, e.g., serine, cysteine, or aspartic acid. Cathepsin D is the main lysosomal aspartic protease and is widely expressed in the brain, including the cortex, hippocampus, and striatum [11]. Tau can be degraded *in vitro* by Cathepsin D [12] and experiments using cell models show that lysosomes are involved in the degradation of tau [7, 9]. Also, Cathepsin D upregulation has been described in AD and its extracellular presence in senile plaques was clearly noted [13].

In order to study the mechanisms underlying tau pathology *in vivo*, the TauVLW transgenic mouse line was generated as a model of tauopathy. This transgenic mouse line expresses the longest central nervous system isoform of human tau carrying the three FTDP-17 missense mutations G272V, P301L, and R406W under the control of the *thy1* promoter to direct neuron-specific expression. Although they do not appear to suffer altered memory functions [14], TauVLW mice develop filamentous tau aggregates and lysosomal/endosomal abnormalities in hippocampal and cortical regions [15].

In the present work, we have analyzed the levels and localization of human mutant tau in the hippocampus of TauVLW mice at three different ages. In addition, we have studied Cathepsin D localization in the same brain and at the same three ages, comparing wild type mice with transgenic mice. In order to determine tau localization in lysosomal compartments, we have performed co-localization experiments using the confocal microscope, ultrastructural studies, lysosomal fraction analysis in the hippocampus of transgenic mice. Our data suggest that part of the human mutant tau in the hippocampus of transgenic mice could be degraded inside lysosomes by Cathepsin D.

## MATERIALS AND METHODS

### Animals

Detailed characterizations of TauVLW mouse lines have been previously published [15]. In brief, the TauVLW line overexpresses the largest human tau isoform of the central nervous system containing the two N-terminal inserts, four microtubule-binding repeat elements, and three FTDP-17-linked mutations (G207V, P301L, and R406W) driven by the mouse *thy1* promoter in the C57BL6jxCBA hybrid background.

Wild type mice belong to the C57BL6j background. This work used a total of 25 transgenic mice and 18 wild type mice aged 1.5, 3, and 24 months old. Some mice were intraperitoneally anesthetized with a pentobarbital solution and perfused with 4% paraformaldehyde in phosphate buffered saline (PBS) pH 7.4 before postfixing

their brains by immersion 24 h in the same fixative for immunohistochemical studies. Brains for electron microscopy study were fixed by perfusion with 4% paraformaldehyde (Panreac) and 0.2% glutaraldehyde (MERK) in PBS. After washing in PBS, brains were sectioned at 30  $\mu$ m in the sagittal plane on a vibrotome (Lancer). Sections were stained with thionine or immunostained with different antibodies. For the western blot studies, other mice were killed and their brains rapidly removed and frozen at  $-80^{\circ}\text{C}$  until use. All animals were bred at the Centro de Biología Molecular "Severo Ochoa" (Madrid, Spain). Four or five mice were housed per cage, with food and water ad libitum, in a temperature-controlled environment with a normal dark-light cycle (12 h of light/12 h of dark). Animals were handled according to the European Union guidelines (86/609/ECC) approved by the Bioethics Commission of the Universidad Autónoma de Madrid, so as to minimize their suffering and to reduce the number of animals to the minimum.

### Antibodies

The following primary antibodies were used: mouse monoclonal anti-human tau HT7 (Thermo Scientific, USA), goat polyclonal anti-Cathepsin D R-20 (Santa Cruz Biotechnology, California), rabbit polyclonal anti-Cathepsin D (Calbiochem, Germany), rabbit polyclonal anti-LAMP-2 (Igp96; Invitrogen, CA), mouse monoclonal anti-actin (SIGMA), rabbit polyclonal anti-TOM20 (translocase of outer mitochondrial membranes, sc-11415; Santa Cruz Biotechnology, California) and anti-GADPH (ABCAM; Cambridge, UK). Sources of other commercial antibodies were as follows. Secondary horseradish peroxidase anti-goat and biotinylated secondary antibody were obtained from Santa Cruz Biotechnology. Alexa-conjugated secondary antibodies were purchased from Invitrogen. Secondary horseradish peroxidase anti-mouse was from DAKO (Denmark) and streptavidin-peroxidase from Biomakor. Colloidal gold (1 nm)-labeled Goat-anti-Mouse IgG Ultra-Small from AURION (The Netherlands).

### Western blot analysis

Extracts from hippocampi of transgenic and wild type mice (1.5-, 3-, and 24-months-old) were prepared by homogenizing in ice-cold lysis buffer (20mM HEPES, pH 7.4, 100mM NaCl, 50mM NaF, 5mM EDTA, 1% Triton X-100, 1mM sodium orthovanadate, 1mM pyrophosphates, 0.1mM molybdic acid, and protease inhibitor cocktail (COMPLETE, Roche).

The protein concentration of samples was determined using the Bradford assay [16]. Total protein (10–50 $\mu$ g) was electrophoresed on 12% or 10% SDS-PAGE for Cathepsin D or for tau, respectively, and electrophoretically transferred to a nitrocellulose membrane (PROTRAN, Whatman). The experiments were performed using the following primary antibodies: anti-Cathepsin D R-20 (0.7 $\mu$ g/ml), anti-human tau HT7 (1:5000–1:10000) and anti-actin (1:10000).

The membranes were incubated with the antibody overnight at  $4^{\circ}\text{C}$  in 3% BSA in PBS and 0.1% Tween 20. After four rinses/washes, the membrane was incubated with a

horseradish peroxidase anti-goat (1:4000) or anti-mouse (1:5000–1:10000) IgG conjugate, followed by several washes in PBS-Tween20. The immunoreactive proteins were visualized using a Western Lightning Plus-ECL (Perkin Elmer Life Sciences, MA USA). Each western blot was repeated at least three times. Blots were quantified using the EPSON Perfection 1660 scanner and the ImageJ 1.46r image analysis system. The levels of various markers were normalized to the -actin present in each band.

### Immunohistochemistry

Sagittal sections of transgenic and wild type mice of different ages were processed free floating using the biotin-streptavidin-peroxidase method, with diaminobenzidine (DAB) as a chromogen. Endogenous peroxidase was inactivated by incubating sections in a solution of 0.3% hydrogen peroxide in methanol for 30 min. Sections were then incubated in 10% normal horse or rabbit serum in phosphate buffered saline for 1 h. The following antibodies were used: anti-Cathepsin D R-20 (1:200) and anti-human tau HT7 (1:250), overnight at 4°C. Next day, the sections were incubated with the corresponding biotinylated secondary antibody (1:200) at room temperature for 1 h, followed by streptavidin-peroxidase (1:1200) at room temperature for 1 h. In order to rule out non specific staining, preabsorption of secondary antibody was performed with additional sections, for 24 h at 4°C. To evaluate the specificity of the primary antibody staining adjacent sections were incubated in vehicle solution without the primary antibody. For light microscopy, some immunostained sections were with thionine. The sections were examined and photographed in a NIKON light microscope.

For electron microscopy, sections were postfixated in 2% OsO<sub>4</sub> for 1 h, dehydrated, embedded in araldite, and mounted in Formvar-coated slides using plastic coverslips. After polymerization, selected areas of hippocampus were photographed, trimmed and resectioned at 1.5 μm. These semithin sections were rephotographed and resectioned in ultrathin sections (60–40 nm). The ultrathin sections were examined in a Jeol 301 electron microscope without heavy metal staining to avoid artifactual precipitates. Double immunofluorescence and confocal microscopy in brain sections

Additional vibratome sections were processed for double-immunofluorescence labelling. Non-specific binding sites were blocked with 10% normal donkey serum in PBS at room temperature. The sections were incubated at 4°C overnight with anti-Cathepsin D (1:500; Calbiochem) and with anti-human tau HT7 (1:1000). After washing in PBS, the sections were incubated in the dark with the mixture of secondary antibodies: Alexa 488-conjugated anti-rabbit and Alexa 555-conjugated anti-mouse (1:400, Invitrogen) for 45 min at room temperature. After washing in PBS, sections were stained with a saturated solution of Sudan black B (SIGMA, Spain) for 30 min to block autofluorescence, rinsed in 70% ethanol and washed in distilled water. The sections were mounted in Prolong Mounting medium (Molecular Probes), sealed, and dried overnight. The specificity of the labeling confirmed by incubation of sections with the secondary antibody, omitting the primary antibody. No immunoreactivity was observed under these conditions.

## Colocalization analysis

Confocal images were obtained using a TCS SP5 Spectral Leica Confocal microscope using an oilimmersion 63X objective with sequential-acquisition setting. The detector pinholes were set to give a 0.3 $\mu$ m optical slice (lysosomal average size is 0.5–1.5  $\mu$ m). Comparisons of the degree of colocalization between tau and Cathepsin D were performed on stacks using orthogonal projection in merged panels with a Leica LAS AF software. Subcellular fractionation Hippocampus from TauVLW and wild type mice (three 1.5-month-old animals per group) were homogenized in cold 0.3 mol/L sucrose in PBS with protease vanadate, 1mMpyrophosphates, 0.1mMokadaic acid, and protease inhibitor cocktail (COMPLETE, Roche).

The protein concentration of samples was determined using the Bradford assay [16]. Total protein (10–50g) was electrophoresed on 12% or 10% SDS-PAGE for Cathepsin D or for tau, respectively, and electrophoretically transferred to a nitrocellulose membrane (PROTRAN, Whatman). The experiments were performed using the following primary antibodies: anti-Cathepsin D R-20 (0.7g/ml), anti-human tauHT7 (1:5000–1:10000) and anti--actin (1:10000).

The membranes were incubated with the antibody overnight at 4°C in 3% BSA in PBS and 0.1% Tween 20. After four rinses/washes, the membrane was incubated with a horseradish peroxidase anti-goat (1:4000) or anti-mouse (1:5000–1:10000) IgG conjugate, followed by severalwashes in PBS-Tween20.The immunoreactive proteinswere visualized using aWestern Lightning Plus-ECL (Perkin Elmer Life, Sciences, MA USA). Each western blot was repeated at least three times.

Blots were quantified using the EPSON Perfection 1660 scanner and the ImageJ1.46r image analysis system. The levels of various markers were normalized to the -actin present in each band.

## Immunohistochemistry

Sagittal sections of transgenic and wild type mice of different ages were processed free floating using the biotin-streptavidin-peroxidase method, with diaminobenzidine (DAB) as a chromogen. Endogenous peroxidasewas inactivated by incubating sections in a solution of 0.3% hydrogen peroxide in methanol for 30min. Sections were then incubated in 10% normal horse or rabbit serum in phosphate buffered saline for 1 h. The following antibodies were used: anti-Cathepsin D R-20 (1:200) and anti-human tau HT7 (1:250), overnight at 4°C. Next day, the sections were incubated with the corresponding biotinylated antibody (1:200) at room temperature for 1 h, followed by streptavidin-peroxidase (1:1200) at room temperature for 1 h. In order to rule out non specific staining, preabsorption of secondary antibody was performed with additional sections, for 24 h at 4°C. To evaluate the specificity of the primary antibody staining adjacent sections were incubated in vehicle solution without the primary antibody. For light microscopy, some immunostained sections were counterstained with thionine. The sections were examined and photographed in a NIKON light microscope.

For electron microscopy, sections were postfixated in 2% OsO<sub>4</sub> for 1 h, dehydrated, embedded in araldite, and mounted in Formvar-coated slides using plas-200 coverslips. After polymerization, selected areas of hippocampus were photographed, trimmed and resectioned at 1.5 μm. These semithin sections were rephotographed and resectioned in ultrathin sections (60–40 nm). The ultrathin sections were examined in a Jeol 301 electron microscope without heavy metal staining to avoid artifactual precipitates. Double immunofluorescence and confocal microscopy in brain sections  
Additional vibratome sections were processed for double-immunofluorescence labelling. Non-specific binding sites were blocked with 10% normal donkey serum in PBS at room temperature. The sections were incubated at 4°C overnight with anti-Cathepsin D (1:500; Calbiochem) and with anti-human tauHT7 (1:1000). After washing in PBS, the sections were incubated in the dark with the mixture of secondary antibodies: Alexa 488-conjugated anti-rabbit and Alexa 555-conjugated anti-mouse (1:400, Invitrogen) for 45 min at room temperature. After washing in PBS, sections were stained with a saturated solution of Sudan black B (SIGMA, Spain) for 30 min to block autofluorescence, rinsed in 70% ethanol and washed in distilled water. The sections were mounted in Prolong Mounting medium (Molecular Probes), sealed, and dried overnight. The specificity of the labeling was confirmed by incubation of sections with the secondary antibody, omitting the primary antibody. No immunoreactivity was observed under these conditions.

#### Colocalization analysis

Confocal images were obtained using a TCS SP5 Spectral Leica Confocal microscope using an oilimmersion 63X objective with sequential-acquisition setting. The detector pinholes were set to give a 0.3 μm optical slice (lysosomal average size is 0.5–1.5 μm). 236

Comparisons of the degree of colocalization between tau and Cathepsin D were performed on stacks using orthogonal projection in merged panels with a Leica LAS AF software. 240

Subcellular fractionation Hippocampus from TauVLW and wild type mice (three 1.5-month-old animals per group) were homogenized in cold 0.3 mol/L sucrose in PBS with protease inhibitors. Homogenates were centrifuged at 700 g to pellet the nuclei and intact cell debris. Supernatant was centrifuged at 10,000 g for 10 min to sediment the crude lysosomal-mitochondrial fraction which was re-homogenized in 10 ml of 300 mmol/L sucrose, containing 1 mmol/L CaCl<sub>2</sub>. The new homogenate was incubated at 37°C for 5 min for mitochondria swallowing; after adding 10 ml of 50% Percoll solution the homogenate was centrifuged at 10,000 g for 10 min to obtain the lysosomal fraction. Fractions were equalized and immunoblotted with anti-LAMP2 (1:2000), anti-Cathepsin D R-20 (0.7 g/ml), HT7 (1:1000), anti-TOM 20 (1:1000), and anti-GADPH (1:5000) antibodies. Membranes were incubated with appropriate horseradish peroxidase-conjugated secondary antibodies (1:2000), and visualized using an ECL detection kit.

Double-labeling immunohistochemistry Immunoperoxidase detection of Cathepsin D followed by immunogold–silver detection of tau using a pre-embedding immunoperoxidase and immunogold–silver labeling method previously described by Sirerol-Piquer et al. [17]. As the primary antisera against Cathepsin D and tau were raised in goat and mice, respectively, recognition could be achieved by utilization of appropriate species-specific antibodies. All the incubations were carried out at room temperature with continuous on a rotator. The sections were placed in 0.1 M phosphate-buffer (PB) containing 1% sodium borohydride to inactivate residual aldehyde groups in the tissue sections. Sections were then washed with 0.1 M PB several times until the solution was clear of bubbles. Sections were then incubated in 10% normal horse serum in 0.1 M Tris-buffered saline (TBS) for 1 h. After blocking, the sections were incubated in a mixture of anti-Cathepsin D R-20 (1:200) and anti-human tau HT7 (1:250), overnight at 4°C. In negative control experiments, sections were processed for dual peroxidase and gold labeling with omission of either one or both antisera.

For immunoperoxidase visualization of Cathepsin D, we used the biotin-streptavidin-peroxidase method, with diaminobenzidine (DAB) as a chromogen. Following the incubation in primary antisera, the sections were incubated in secondary biotinylated horse antigoat IgG (1:200, Vector Laboratories, Burlingame, CA, USA) for 1 h and followed by streptavidinperoxidase (1:1200) at room temperature for another hour. After the peroxidase reaction was completed, the sections were transferred to 0.01 M PBS, and subsequently incubated for 10 min in 0.8% BSA and 0.1% gelatin in PBS, a blocking step to minimize nonspecific binding of gold particles to tissue.

For immunogold–silver labeling, the sections were then incubated for 2 h in colloidal gold (1 nm)-labeled goat anti-mouse IgG (1:50) and fixed for 10 min in 2% glutaraldehyde in 0.01 M PBS. Incubation in 0.2 M sodium citrate buffer prior to silver intensification of the bound gold particles was used to remove phosphate ions which could result in precipitation of silver particles. Then, sections were reacted with a silver solution R-GENT-SE-EM kit (AURION) for 4–8 min for electron microscopy.

For electron microscopy, selected immunolabeled sections were fixed as described above. 310

#### Data analysis

Data obtained by densitometry were descriptively analyzed with Excel and are presented as the mean±SEM from a minimum of three separate experiments.

Data were analyzed by the Shapiro-Wilk test to determine if the variables follow a normal distribution with the R2.14.0 program. Normal variables were subjected to Student's t-test and non-normal variables were subjected to a non-parametric test, the Mann-Whitney U-test, using the SPSS17.0 program for statistical comparison.

Statistical significance was inferred at  $p < 0.05$ .

#### RESULTS

Expression of human TauV<sub>LW</sub> transgenic protein: Immunoblotting analysis In previous work, Lim et al. described the pattern and levels of expression of human mutant tau in the murine model TauV<sub>LW</sub>, using biochemical and immunohistochemical approaches with the human-specific anti-Tau antibody T14 [15]. In the current study, we wanted to confirm the expression of human mutant tau protein in transgenic TauV<sub>LW</sub> mice with a new antibody, HT7. This antibody, which only recognizes human tau, reacted with a peptide corresponding to the transgene product (Fig. 1A). Hippocampus of TauV<sub>LW</sub> mice at 1.5, 3, and 24 months of age was dissected out and human tau protein levels were examined in the extracts by western blot. The difference in the total protein amount between the samples was normalized by  $\alpha$ -actin band intensity. The hippocampus of TauV<sub>LW</sub> mice showed an increase in the human tau levels at 3-months-old as compared to 1.5-months-old (Fig. 1B,  $***344 p = 0.0001$ ). These results agree with those obtained by Lim and coworkers using the same animal model 1.5- and 5.5-months-old [15]. Aging is a known risk factor for neurodegenerative disorders; therefore we completed the study by analyzing human mutant tau levels in 24-months-old mice (Fig. 1A). The data revealed significant differences between mice at 24 and 1.5 months of age ( $**351 p = 0.001$ ), but no statistically significant differences were observed as compared with 3-months-old mice (Fig. 1B). These results suggest that human mutant tau had reached the peak of its expression at 3 months of age in the TauV<sub>LW</sub> mice. We could conclude that results obtained with HT7 antibody are consistent with previous studies performed with T14 antibody in the same murine model and, also, we extended the study to 24 months of age.

Expression of human TauV<sub>LW</sub> transgenic protein: Immunohistochemistry analysis We next evaluated expression of human mutant tau by immunohistochemical experiments with HT7 antibody in vibratome sagittal brain sections from 1.5- and 24-months-old wild type and TauV<sub>LW</sub> mice (Fig. 1C-H). Wild type mice showed no staining, which revealed the high specificity of the HT7 antibody, indicating that it does not recognize murine tau (Fig. 1C, F). In the hippocampus of TauV<sub>LW</sub> mice, we observed a somatodendritic staining of human mutant tau with HT7 antibody at all ages studied. In the hippocampus of 1.5-months-old transgenic mice, staining of most neuronal cell bodies and apical dendrites of pyramidal neurons of CA1 and CA3 but not CA2 hippocampal sector (Fig. 1D) neurons was enhanced, as also reported by Lim and coworkers using the T14 antibody in TauV<sub>LW</sub> mice [15]. The absence of staining in CA2 may be due to strong transgenic position-effect variegation, since a Thy1-driven transgene is often stochastically and differentially expressed in subsets of neurons in different transgenic lines [18, 19].

Pyramidal neurons in sector CA1 contained the highest amounts of TauV<sub>LW</sub> limited to cell bodies. Granule cells of the dentate gyrus showed a lower staining with HT7 antibody (Fig. 1D), although mossy fibers projecting to CA3 showed intense staining (see arrow in Fig. 1D). The level of immunostaining with HT7 antibody in CA1 is similar at 1.5- and 24-months old (Figs. 1D, G), but it is stronger in mossy fibers of 24-months-old mice (see arrow in Fig. 1G). The thionine staining revealed no differences in any

hippocampal sector when 1.5- or 24-months-old TauVLW mice (Fig. 1E, H) were compared, indicating no neuronal loss.

Cathepsin D analysis in hippocampus of wild type and transgenic TauVLW mice:  
Immunoblotting analysis

Previous observations of Lim and coworkers demonstrated an increased number of lysosomes in neurons of TauVLW mice brains compared to wild-type animals at the same age [15]. To determine the possible involvement of lysosomal enzymes in the alterations observed in transgenic mice, we focused our study on Cathepsin D, evaluating its levels in the hippocampus of 1.5-, 3-, and 24-months-old TauVLW mice compared to wild type mice (Fig. 2A, B).

In the hippocampus, data from western blot using R-20 antibody, which recognizes Cathepsin D, showed an increase of Cathepsin D levels in transgenic mice compared to wild type mice (Fig. 2A). This enhancement was maintained at all ages studied, as revealed by the statistical data analysis ( $***p = 0.0001$ ) (Fig. 2B). In wild type mice, Cathepsin D levels remained almost constant at 1.5- and 3-months-old, but a significant decrease was observed at 24-months-old (Fig. 2B).

Together, these results showed the level of expression of Cathepsin D in hippocampus at all ages is higher in the transgenic mice than in the wild type mice, probably as a consequence of an increase in human mutant tau.

Cathepsin D analysis in hippocampus of wild type and transgenic TauVLW mice:  
Immunohistochemical analysis

To analyze the distribution and cellular localization of Cathepsin D in the hippocampus in wild type and transgenic mice, we performed immunohistochemistry with the same R-20 antibody used in the western blot analysis (Fig. 2A). Our results indicated that this anti-body has a great specificity, since no immunoreactivity was detected when the primary antibody was omitted (data not shown). Cathepsin D immunoreactivity was widely distributed in neurons of the hippocampus in sagittal sections of 1.5- and 24-months-old wild type and transgenic mice (Fig. 2C–J). Immunohistochemical analysis of hippocampus from TauVLW mice showed greater Cathepsin D immunoreactivity than did wild type mice at the ages studied (Compare Figs. 2C with 2D and 2E with 2F), thus confirming the results obtained in the Cathepsin D western blot analysis

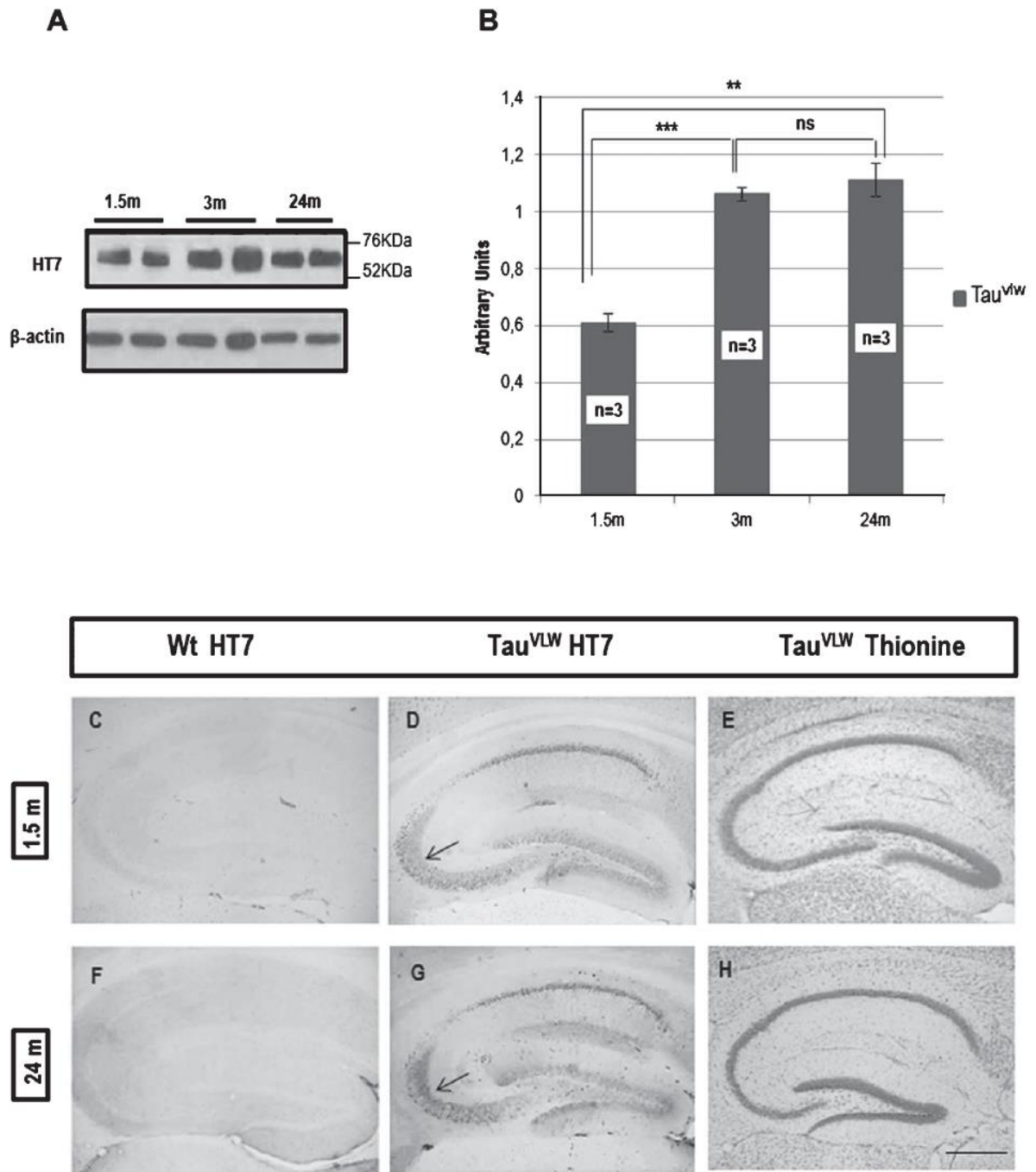


Fig. 1. Analysis of human mutant Tau protein in transgenic Tau<sup>VLW</sup> mice. A) Extracts from the hippocampus of 1.5-, 3-, and 24-months-old transgenic Tau<sup>VLW</sup> mice were probed with anti-Tau antibody HT7 and  $\beta$ -actin as a control of protein loading. B) Quantification by densitometry of the data from (A) showing the mean values and typical error from at least three separate experiments, each of which was replicated three or more times ( $***p = 0.0001$ ,  $**p = 0.001$ , ns = non-significant, Mann-Whitney-U test). Immunohistochemistry in hippocampal sagittal sections of wild type (C and F) and Tau<sup>VLW</sup> (D and G) mice were performed with antibody HT7. No HT7 immunostaining was observed in hippocampi from 1.5-months-old (C) and 24-months-old (F) wild type mice. Hippocampi from 1.5-months-old (D) and 24-months-old (G) Tau<sup>VLW</sup> mice revealed high transgene expression in most neuronal cell bodies and apical dendrites of pyramidal neurons in the CA1 and CA3, but not CA2 hippocampal sectors. Arrows in panels D and G show mossy fibers stained with HT7 antibody. Sagittal sections from hippocampi of 1.5-months-old (E) and 24-months-old (H) transgenic Tau<sup>VLW</sup> mice were thionine-stained and showed no neuronal loss. Scale bar = 500 nm.

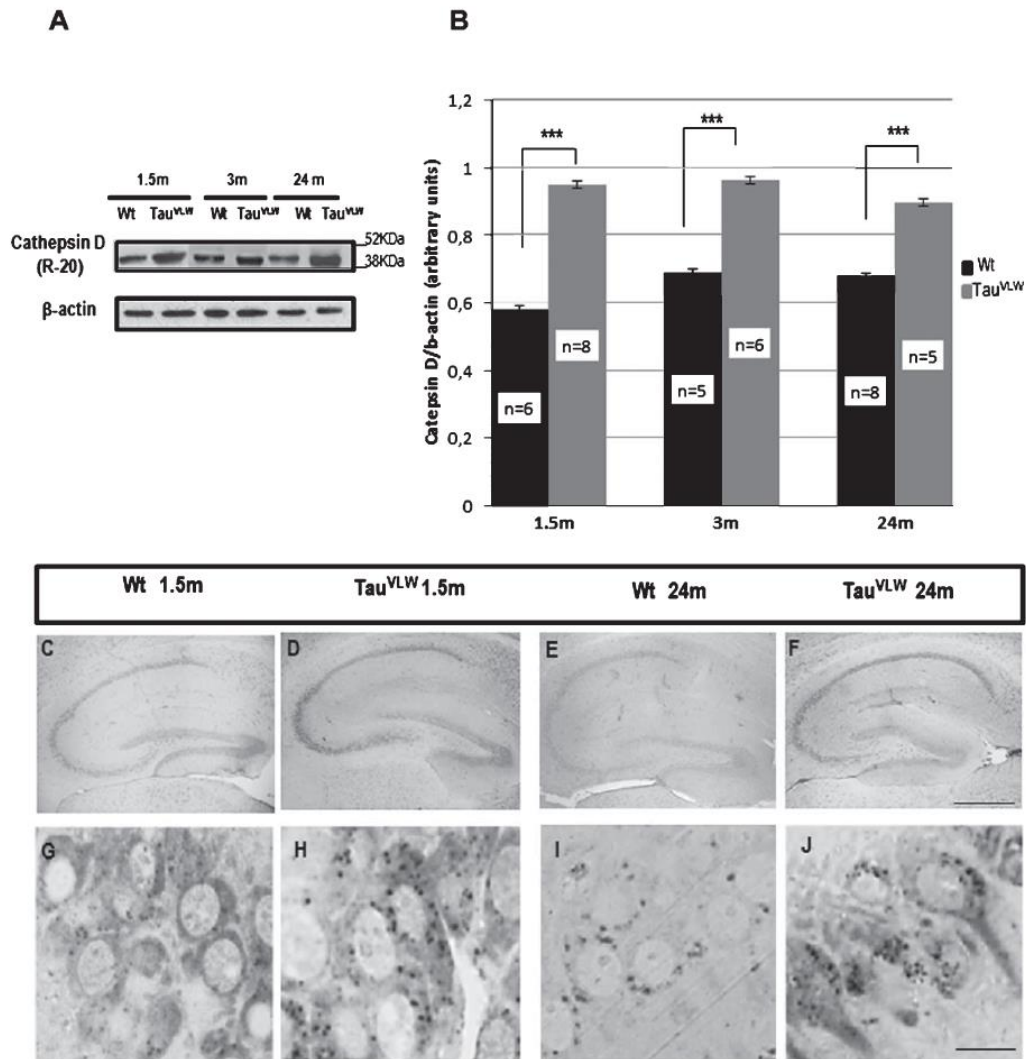


Fig. 2. Analysis of Cathepsin D of wild type and transgenic Tau<sup>VLW</sup> mice at different ages. A) Extracts from hippocampus of wild type and transgenic Tau<sup>VLW</sup> were probed with anti-Cathepsin D antibody (R-20) and with  $\beta$ -actin as a control for protein loading. B) Quantification by densitometry of the data from (A). Wild type (black bars) and transgenic Tau<sup>VLW</sup> mice (grey bars) showing the mean values and typical error from at least three separate experiments, each of which was repeated three or more times (\*\*\*)  $p = 0.0001$ , Mann-Whitney-U test). Immunohistochemistry in hippocampal sagittal sections of 1.5-months-old (C) and 24-months-old (E) wild type and 1.5-months-old (D) and 24-months-old (F) transgenic Tau<sup>VLW</sup> mice were performed with R20 antibody against Cathepsin D. A semithin section from CA3 sector of hippocampus of 1.5-months-old (G) or 24-months-old wild type (I), and 1.5-months-old (H) or 24-months-old transgenic Tau<sup>VLW</sup> mouse (J) immunostained with the same Cathepsin D antibody. Note the presence of a punctuated immunolabeling corresponding to lysosomal staining. C, D, E, and F, Scale bar = 500 nm. G, H, I, and J, Scale bar = 10  $\mu$ m.

(Fig. 2A). Pyramidal neurons of CA1, CA2 (not stained with HT7), and CA3 exhibited intense Cathepsin D immunostaining. At higher magnifications, semithin sections from sector CA3 of the hippocampus revealed a punctuated or granular immunolabeling within the cytoplasm around the nucleus in most of the neurons, corresponding to lysosomal staining (Fig. 2G–J). Also, there was a diffuse pattern in the

nucleus and cytoplasm in wild type and transgenic mice. At 1.5 months of age, neurons from CA3 of TauV<sup>LW</sup> mice presented

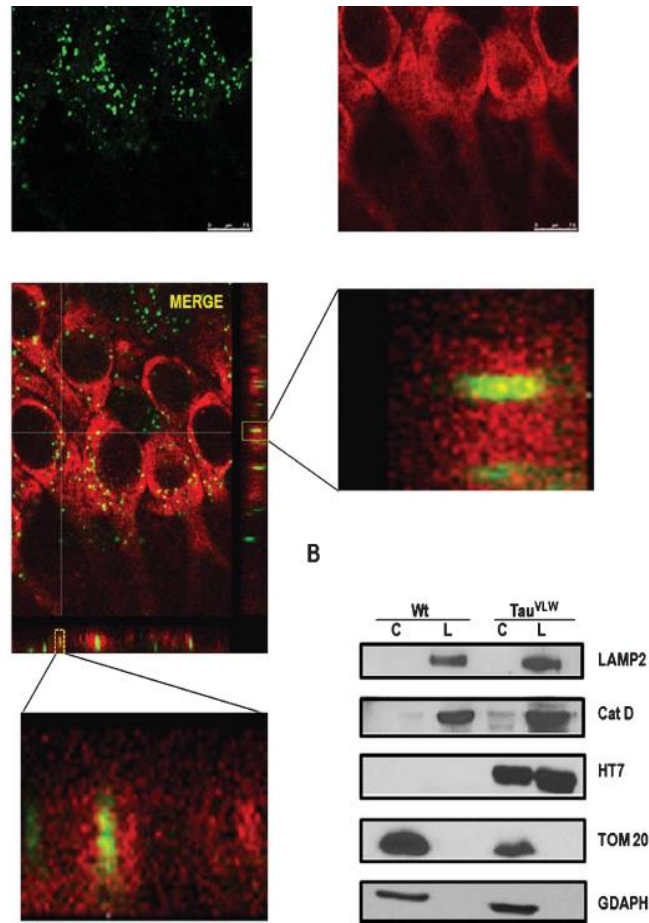


Fig. 3. Analysis of Cathepsin D in Tau<sup>V<sup>LW</sup></sup> mice by confocal microscopy. A) Sections from CA1 hippocampal sector of 1.5-months-old Tau<sup>V<sup>LW</sup></sup> mice were incubated with antibodies against Cathepsin D and human mutant tau. Representative double immunofluorescence photomicrographs of distribution of the Cathepsin D (Cat D, green) and Tau (HT7, red) in the CA1 hippocampal sector from 1.5-months-old Tau<sup>V<sup>LW</sup></sup> mice is shown. In some cases, tau staining was colocalized with Cathepsin D-positive neurons (MERGE, and inset). Orthogonal projections in merged panel confirm co-localization of tau with Cathepsin D. Imaging was performed using a TCS SP5 Spectral Leica Confocal microscope. Scale bar: 75 μm. B) Subcellular fractionation of hippocampus from 1.5-months-old Wt and Tau<sup>V<sup>LW</sup></sup>. Cytosolic (C) and lysosomal (L) fractions were prepared according to Material and Methods. Western blot against lysosome membrane protein (LAMP2), Cathepsin D protein and human tau protein (HT7), mitochondrial protein TOM20, and cytosolic protein GDAPH, show part of human mutant tau in lysosomal fraction.

a stronger granular staining than the wild type mice (Fig. 2G, H). Interestingly, some pyramidal neurons from CA3 of 24-months-old TauV<sup>LW</sup> mice showed lysosomes around the nucleus (Fig. 2J).

Together these findings suggest that the distribution pattern of Cathepsin D observed in the hippocampus of TauV<sup>LW</sup> mice matches the regions where human mutant tau accumulates, probably as consequence of an increase of exogenous tau.

Colocalization of human mutant tau with Cathepsin D in hippocampus of TauV<sup>LW</sup> mice

In the present work, hippocampus from 1.5-months old TauV<sup>LW</sup> mice showed a marked expression of human mutant tau, mainly in sectors CA1 and CA3. Furthermore, the hippocampus of 1.5-months old TauV<sup>LW</sup> mice exhibited intense Cathepsin D immunoreactivity (Fig. 2C–J) and increased protein levels (Fig. 2A–B). Confocal analysis

of double immunofluorescence staining with an antibody against Cathepsin D and the HT7 antibody against human tau were performed. The Cathepsin D-positive granular structures scattered in the soma of all neurons indicate its localization within lysosomes (Fig. 3, Cat D). The human mutant tau exhibited somatodendritic localization (Fig. 3, HT7). In merged confocal image of a single optical section (Image 25 of Supplementary Fig. 1), part of the human tau colocalized with Cathepsin D-positive vesicles in some CA1 neurons from 1.5-months-old TauVLW mice (Fig. 3, MERGE).

Orthogonal projections of confocal merge images of Cathepsin D and TauVLW confirm this partial colocalization (see areas indicated by the rectangles in Fig. 3A). Double immunofluorescence images of each optical section could be observed in Supplementary Fig. 1. Similar results were obtained with CA3 neurons (data not shown).

To investigate if this colocalization of TauVLW with Cathepsin D observed by confocal microscopy occurs in lysosomes, we performed subcellular fractionation and immunoblotting analysis in the hippocampus of 1.5-months-old TauVLW and age-matched control mice. The purity of lysosomal fractions isolated from both groups of animals was confirmed by its reaction with the specific lysosomal antibodies Cathepsin D and LAMP2 (Fig. 3B). The lack of reaction with the specific mitochondrial (TOM 20) or cytoplasmic (GADPH) antibodies confirms the purity of lysosomal fraction (Fig. 3B). Our results revealed that part of the TauVLW (stained with monoclonal antibody HT7; Fig. 3B) was in the lysosomal fraction. All these data suggest that some transgenic tau was already located in lysosomal compartments at early ages.

#### Ultrastructural analysis of TauVLW mice

To better define the subcellular location of human mutant tau, we performed electron microscopy studies in the hippocampus of TauVLW mice using the HT7 antibody.

At light microscope resolution, no HT7 immunoreactivity was observed in a semithin section of CA1 sector from wild type mice (Fig. 4A1), but HT7 immunostaining was very strong in the same neuronal populations in TauVLW mice (Fig. 4B1).

At the ultrastructural level, several HT-7 immunopositive multivesicular bodies (MVB) were observed in the cytoplasm of HT7-positive CA1 hippocampal pyramidal neurons from 3-months-old TauVLW mice (Fig. 4B2). These immunopositive MVB showed vesicles homogeneously filled with immunoprecipitate as well as patches of reaction product over the cytoplasmic side of the MVB membrane (Fig. 4B3-5). We never found these immunostained MVB in wild type animals (Fig. 4A2).

In order to confirm the presence of TauVLW in lysosomes, we performed immunogold electron microscopy. Fig. 5 shows a representative image of a vesicle containing Cathepsin D-positive electron-dense material and tau immunogold particles. We did not find this tau immunogold staining in wild type animals (Supplementary Fig. 2).

These electron microscope images showing the presence of both tau and Cathepsin D within MVB are compatible with the idea that part of human transgenic tau is localized in this particular lysosomal compartment, where it could be degraded.

## DISCUSSION

Although tau plays an important role in the pathology of tauopathies, the mechanisms involved are not entirely understood. The use of animal models is a powerful tool to study some aspects of the neuropathology of these diseases. In a murine model of tauopathy, TauVLW mice, we previously reported that overexpression of human mutant tau results in hyperphosphorylation of the transgenic tau, which accumulates in insoluble tau polymers, accompanied increases in the number of lysosomes, which, moreover, display aberrant morphology [15, 20, 21]. In the present study using HT7 antibody, we observed a somatodendritic accumulation of human mutant tau

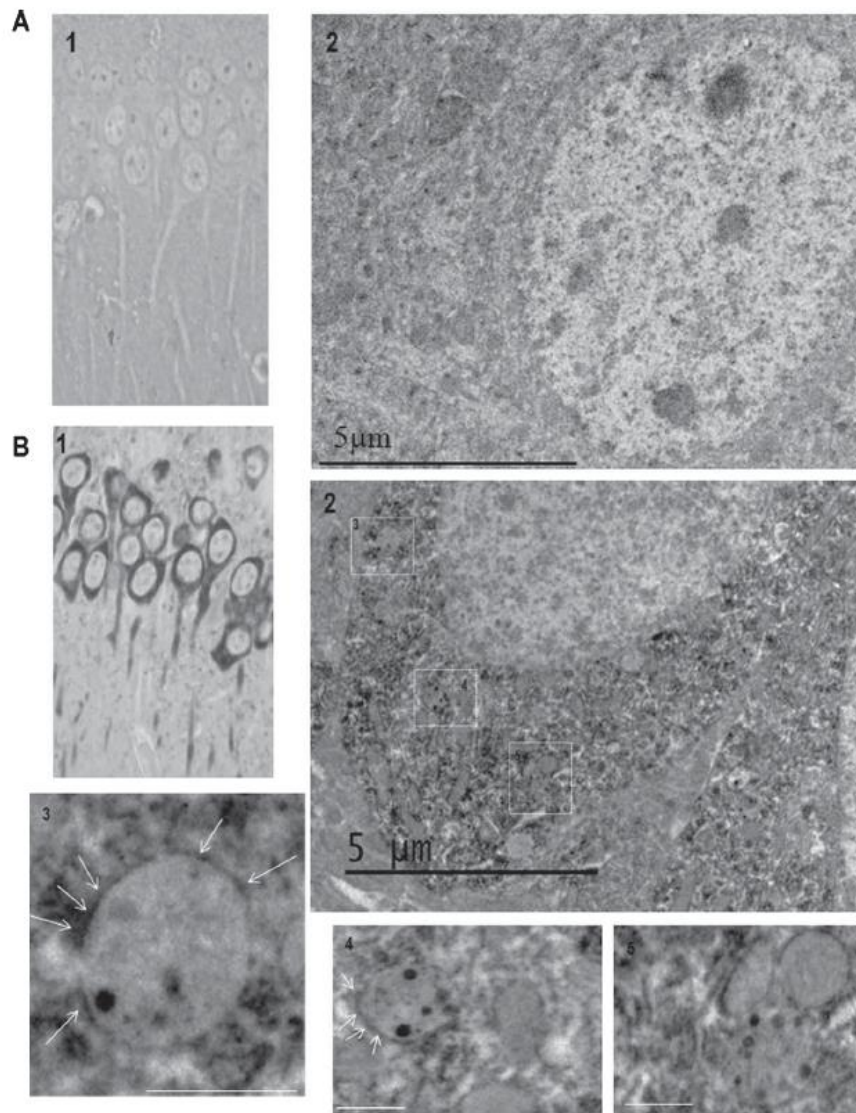


Fig. 4. Ultrastructural analysis of hippocampus from wild type and  $\text{Tau}^{\text{VLW}}$  mice. A1) A 1- $\mu\text{m}$ -semithin section from CA1 sector of hippocampus from 3-months-old wild type mouse immunostained with the HT-7 antibody. A2) Ultrathin section from the cerebral CA1 sector of hippocampus from 3-months-old wild type mouse immunostained with the HT-7 antibody showing a pyramidal neuron without immunoprecipitate. B1) A 1- $\mu\text{m}$ -semithin section from CA1 sector of hippocampus from  $\text{Tau}^{\text{VLW}}$  mouse immunostained with the HT-7 antibody. B2) Ultrathin section from the cerebral CA1 sector of hippocampus from 3-months-old  $\text{Tau}^{\text{VLW}}$  mouse immunostained with the HT-7 antibody showing two pyramidal neurons with immunoprecipitate. The areas indicated by the rectangles (insets) show HT7 immunopositive multivesicular bodies (MVB) at higher magnification. In addition to immunopositive vesicles, there are patches of reaction product over the cytoplasmic side of the MVB membrane (white arrows). Scale bar: 5  $\mu\text{m}$  and 0.5  $\mu\text{m}$  in the insets.

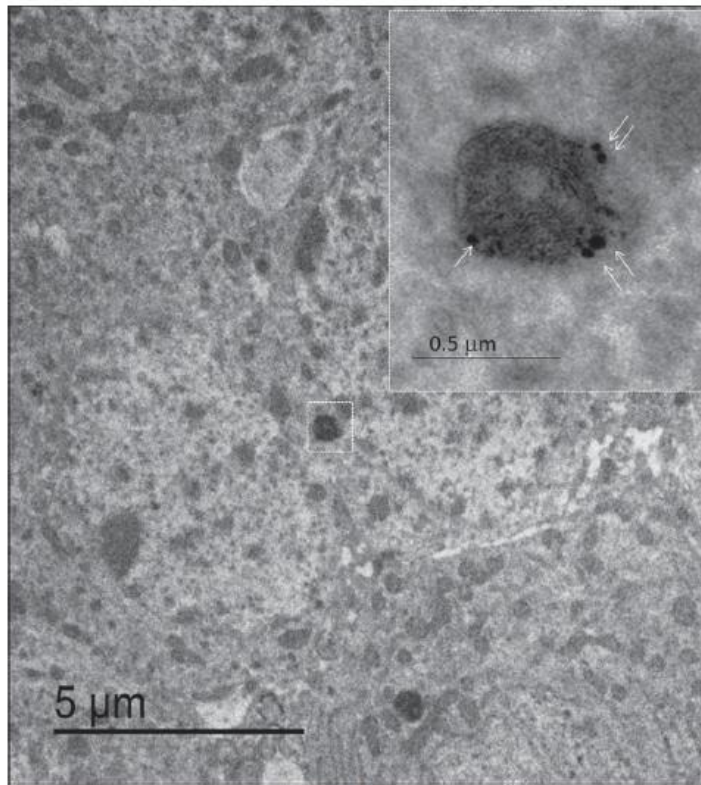


Fig. 5. Existence of tau in lysosome. Ultrathin section from the cerebral CA1 sector of hippocampus from 3-months-old Tau<sup>VLW</sup> mouse immunostained with the Cathepsin D antibody showing a pyramidal neuron with immunoprecipitate and with the HT-7 antibody. The area indicated by the rectangle (inset) shows Cathepsin D immunopositive lysosome at higher magnification. In addition to immunopositive vesicle, there is HT-7 gold particles in the lysosome (white arrows). Scale bar: 5  $\mu$ m and 1  $\mu$ m in the inset.

in the hippocampus of TauVLW 548 mice. This increase in the cytoplasmic tau concentration could be related to overexpression of the transgene that saturates tau binding capacity in microtubules [22]. Since soluble tau has been suspected of being toxic for neurons [23], degradation mechanisms might be induced in order to clear this toxic tau. Tau could be degraded by the ubiquitin-proteasome system and/or the autophagy-lysosome pathway [5].

The contribution of each of these pathways to tau turnover and which forms of tau are degraded by each pathway is not clear and continuous being under active. It seems that full-length tau is cleared by the proteasome system [24, 25], because pharmacological inhibition of the proteasome showed accumulation of full-length tau. The autophagy-lysosomal pathway appears has been postulated to degrade the mutated and truncated forms of tau protein, some of which have pro-aggregation properties and may induce neurodegeneration [9]. Several evidences indicate that lysosomal proteases such as Cathepsins, seem to be involved in the early stages of AD [26]. Using bio-chemical and immunohistochemical approaches, we demonstrate an increase in Cathepsin D levels in the hippocampus of TauVLW mice as compared with wild type mice (Fig. 2). The hippocampus of TauVLW mice expresses high transgenic tau levels (Fig. 1) which are not degraded and then accumulate. We suggest that this region activates a response to tau accumulation by elevating Cathepsin D levels (Fig.

2). Cathepsin D seems important for degrading mutant tau, as its expression was neuroprotective in a *Drosophila* tauopathy model [27].

Our data from double immunofluorescence experiments in the hippocampus showed that part of HT7 immunoreactivity colocalized with some Cathepsin

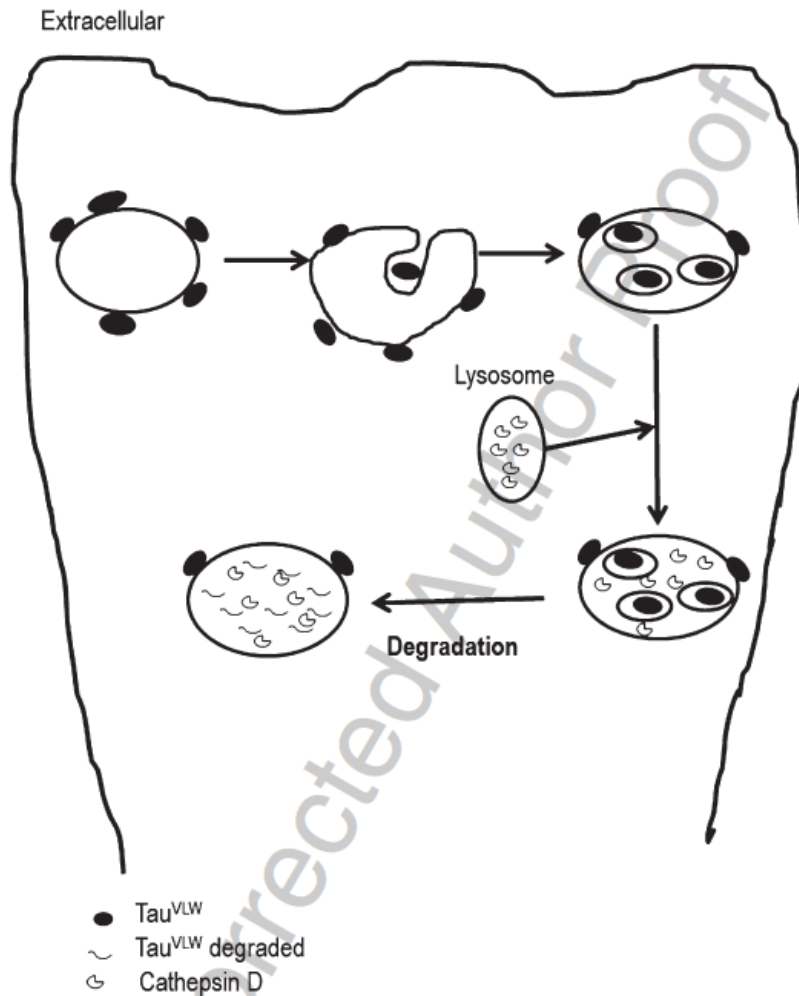


Fig. 6. A possible model of human mutant tau degradation in Tau<sup>VLW</sup> mice. Some human mutant tau is directed to the membrane and internalized into the internal vesicles of multivesicular bodies at an early age. At this point, part of human mutant tau can be degraded after the fusion of multivesicular bodies with lysosomes.

D-positive lysosomes (Fig. 3). Since in our model, the accumulation of mutant tau does not increase with age, one possible interpretation is that in hippocampal neurons, Cathepsin D digests human mutant tau, preventing its further accumulation with age. This also may explain why we did not observe memory impairment in Tau<sup>VLW</sup> mice at older ages [14]. Our results also agree with the report that tau accumulates and forms insoluble aggregates when lysosomal enzymes are inhibited by chloroquine [7].

At the ultrastructural level, HT7 immunoreactivity was observed inside some vesicles within MVBs as well as in small patches over the cytoplasmic side of the membrane of these MVBs (Figs. 4 and 5). Since we also detected Cathepsin D immunoreactivity in

multivesicular bodies (Supplementary Fig. 3), this particular lysosomal structure may be implicated in degrading human mutant tau in this murine model. Fig. 6 shows a model of a possible mechanism explaining how human mutant tau inside MVBs vesicles could be degraded by Cathepsin D in TauVLW mice.

It has been recently described the presence of tau protein in MVB [28] and the exocytosis of those MVBs containing tau vesicles [29]. This mechanism could explain the presence of human mutant tau in brain regions that do not express the tau transgene in TauVLW mice [30] since MVBs have been reported to fuse with the plasma membrane releasing the vesicles to the extracellular space [31].

In conclusion, the increased levels of Cathepsin D observed in our murine model may be a compensatory response to an accumulation of human mutated tau as previously suggested in other studies [32, 33].

We now provide additional data demonstrating that some of the human mutant tau colocalizes with the lysosomal hydrolase Cathepsin D, suggesting that Cathepsin D could be partially responsible for part of tau degradation. Recently, Collin et al. [34] suggest that phosphorylated tau fibrils can bind to and/or get inserted into lysosomes and administration of tau antibody rescues the accumulation of tau pathology.

We also show that human mutant tau accumulates within MVBs in TauVLW mice hippocampal neurons. If MVBs containing human mutant tau fuse with a Cathepsin D lysosome, tau will be degraded. Further experiments are needed to understand how this human mutant tau is cleared in order to develop effective therapeutic approaches.

## **ACKNOWLEDGMENTS**

This study was funded by grant from the Spanish Ministry of Health (SAF 2011-24841).

We are grateful to Pilar Gómez-Ramos and M. Asunción Morán for assistance in article preparation. We are also grateful to Gemma Fuente, Covadonga Aguado and Francisco Urbano for technical assistance. We thank Prof. Jesús Avila de Grado for providing a breeding colony of TauVLW mice.

Authors' disclosures available online (<http://j-alz.com/manuscript-disclosures/14-0456r2>).

## **SUPPLEMENTARY MATERIAL**

The supplementary material is available in the electronic version of this article: <http://dx.doi.org/10.3233/JAD-140456>.

## **REFERENCES**

- [1] Weingarten MD, Lockwood AH, Hwo SY, Kirschner MW (1975) A protein factor essential for microtubule assembly. *Proc Natl Acad Sci U S A* **72**, 1858-1862.
- [2] Spillantini MG, Goedert M (1998) Tau protein pathology in neurodegenerative diseases. *Trends Neurosci* **21**, 428-433.

- [3] Hernandez F, Avila J (2007) Tauopathies. *Cell Mol Life Sci* **64**, 2219-2233.
- [4] Chesser AS, Pritchard SM, Johnson GV (2013) Tau clearance mechanisms and their possible role in the pathogenesis of Alzheimer disease. *Front Neuro* **4**, 122. 657
- [5] Lee MJ, Lee JH, Rubinsztein DC (2013) Tau degradation: The ubiquitin-proteasome system versus the autophagy-lysosome system. *Prog Neurobiol* **105**, 49-59. 660
- [6] Bahr BA, Wisniewski ML, Butler D (2012) Positive lysosomal modulation as a unique strategy to treat age-related protein accumulation diseases. *Rejuvenation Res* **15**, 189-197. 663
- [7] Hamano T, Gendron TF, Causevic E, Yen SH, Lin WL, Isidoro C, Deture M, Ko LW (2008) Autophagic-lysosomal perturbation enhances tau aggregation in transfectants with induced wild-type tau expression. *Eur J Neurosci* **27**, 1119-1130. 667
- [8] Oyama F, Murakami N, Ihara Y (1998) Chloroquine myopathy suggests that tau is degraded in lysosomes: Implication for the formation of paired helical filaments in Alzheimer's disease. *Neurosci Res* **31**, 1-8. 671
- [9] Wang Y, Martinez-Vicente M, Kruger U, Kaushik S, Wong E, Mandelkow EM, Cuervo AM, Mandelkow E (2009) Tau fragmentation, aggregation and clearance: The dual role of lysosomal processing. *Hum Mol Genet* **18**, 4153-4170. 675
- [10] Cataldo AM, Hamilton DJ, Barnett JL, Paskevich PA, Nixon RA (1996) Properties of the endosomal-lysosomal system in the human central nervous system: Disturbances mark most neurons in populations at risk to degenerate in Alzheimer's disease. *J Neurosci* **16**, 186-199. [11] Whitaker JN, Terry LC, Whetsell WO Jr (1981) Immunocytochemical localization of cathepsin D in rat neural tissue. *Brain Res* **216**, 109-124. 683
- [12] Kenessey A, Nacharaju P, Ko LW, Yen SH (1997) Degradation of tau by lysosomal enzyme cathepsin D: Implication for Alzheimer neurofibrillary degeneration. *J Neurochem* **69**, 2026-2038. 687
- [13] Cataldo AM, Nixon RA (1990) Enzymatically active lysosomal proteases are associated with amyloid deposits in Alzheimer brain. *Proc Natl Acad Sci U S A* **87**, 3861-3865. 690
- [14] Ribe EM, Perez M, Puig B, Gich I, Lim F, Cuadrado M, Sesma T, Catena S, Sanchez B, Nieto M, Gomez-Ramos P, Moran MA, Cabodevilla F, Samaranch L, Ortiz L, Perez A, Ferrer I, Avila J, Gomez-Isla T (2005) Accelerated amyloid deposition, neurofibrillary degeneration and neuronal loss in double mutant APP/tau transgenic mice. *Neurobiol Dis* **20**, 814-822. 696
- [15] Lim F, Hernandez F, Lucas JJ, Gomez-Ramos P, Moran MA, Avila J (2001) FTDP-17 mutations in tau transgenic mice provoke lysosomal abnormalities and Tau filaments in forebrain. *Mol Cell Neurosci* **18**, 702-714. 700

- [16] Bradford MM (1976) A rapid and sensitive method for the quantitation of microgram quantities of protein utilizing the principle of protein-dye binding. *Anal Biochem* **72**, 248-254.
- [17] Sirerol-Piquer MS, Cebrian-Silla A, Alfaro-Cervello C, Gomez-Pinedo U, Soriano-Navarro M, Verdugo JM (2012) GFP immunogold staining, from light to electron microscopy, in mammalian cells. *Micron* **43**, 589-599. 707
- [18] Feng G, Mellor RH, Bernstein M, Keller-Peck C, Nguyen QT, Wallace M, Nerbonne JM, Lichtman JW, Sanes JR (2000) Imaging neuronal subsets in transgenic mice expressing multiple spectral variants of GFP. *Neuron* **28**, 41-51. 711
- [19] Young P, Qiu L, Wang D, Zhao S, Gross J, Feng G (2008) Single-neuron labeling with inducible Cre-mediated knock-out in transgenic mice. *Nat Neurosci* **11**, 721-728. 714
- [20] Guerrero R, Navarro P, Gallego E, Garcia-Cabrero AM, Avila J, Sanchez MP (2009) Hyperphosphorylated tau aggregates in the cortex and hippocampus of transgenic mice with mutant human FTDP-17 Tau and lacking the PARK2 gene. *Neuropathol* **117**, 159-168.
- [21] Perez M, Ribe E, Rubio A, Lim F, Moran MA, Ramos PG, Ferrer I, Isla MT, Avila J (2005) Characterization of a double (amyloid precursor protein-tau) transgenic: Tau phosphorylation and aggregation. *Neuroscience* **130**, 339-347.
- [22] Engel T, Lucas JJ, Gomez-Ramos P, Moran MA, Avila J, Hernandez F (2006) Coexpression of FTDP-17 tau and GSK-3beta in transgenic mice induce tau polymerization and neurodegeneration. *Neurobiol Aging* **27**, 1258-1268.
- [23] Avila J, Lucas JJ, Perez M, Hernandez F (2004) Role of tau protein in both physiological and pathological conditions. *Physiol Rev* **84**, 361-384.
- [24] Dolan PJ, Johnson GV (2010) A caspase cleaved form of tau is preferentially degraded through the autophagy pathway. *J Biol Chem* **285**, 21978-21987.
- [25] Liu YH, Wei W, Yin J, Liu GP, Wang Q, Cao FY, Wang JZ (2009) Proteasome inhibition increases tau accumulation independent of phosphorylation. *Neurobiol Aging* **30**, 1949- 1961.
- [26] Nixon RA, Cataldo AM, Mathews PM (2000) The endosomal lysosomal system of neurons in Alzheimer's disease pathogenesis: A review. *Neurochem Res* **25**, 1161-1172.
- [27] Khurana V, Elson-Schwab I, Fulga TA, Sharp KA, Loewen CA, Mulkearns E, Tynnela J, Scherzer CR, Feany MB (2010) Lysosomal dysfunction promotes cleavage and neurotoxicity of tau *in vivo*. *PLoS Genet* **6**, e1001026.
- [28] Simon D, Garcia-Garcia E, Royo F, Falcon-Perez JM, Avila J (2012) Proteostasis of tau. Tau overexpression results in its secretion via membrane vesicles. *FEBS Lett* **586**, 47-54.

[29] Saman S, Kim W, Raya M, Visnick Y, Miro S, Saman S, Jackson B, McKee AC, Alvarez VE, Lee NC, Hall GF (2012) Exosome-associated tau is secreted in tauopathy models and is selectively phosphorylated in cerebrospinal fluid in early Alzheimer disease. *J Biol Chem* **287**, 3842-3849.

[30] Navarro P, Guerrero R, Gallego E, Avila J, Luquin R, Ruiz PJ, Sanchez MP (2008) Memory and exploratory impairment in mice that lack the Park-2 gene and that over-express the human FTDP-17 mutant Tau. *Behav Brain Res* **189**, 350-356.

[31] Harding C, Heuser J, Stahl P (1983) Receptor-mediated endocytosis of transferrin and recycling of the transferrin receptor in rat reticulocytes. *J Cell Biol* **97**, 329-339. 759

[32] Bendiske J, Bahr BA (2003) Lysosomal activation is a compensatory response against protein accumulation and associated synaptopathogenesis—an approach for slowing Alzheimer disease? *J Neuropathol Exp Neurol* **62**, 451-463. 764

[33] Cataldo AM, Barnett JL, Berman SA, Li J, Quarless S, Bursztajn S, Lippa C, Nixon RA (1995) Gene expression and cellular content of cathepsin D in Alzheimer's disease brain: Evidence for early up-regulation of the endosomal-lysosomal system. *Neuron* **14**, 671-680. 769

[34] Collin L, Bohrmann B, Gopfert U, Oroszlan-Szovik K, Ozmen L, Gruninger F (2014) Neuronal uptake of tau/pS422 antibody and reduced progression of tau pathology in a mouse 772

model of Alzheimer's disease. *Brain* **137**, 2834-2846.